

Dimensionality Effects in the Lifetime of Surface States

J. Kliewer,¹ R. Berndt,^{1,2*} E. V. Chulkov,³ V. M. Silkin,³
P. M. Echenique,³ S. Crampin⁴

A long-standing discrepancy between experimental and theoretical values for the lifetimes of holes in the surface-state electron bands on noble metal surfaces is resolved; previous determinations of both are found to have been in error. The ability of the scanning tunneling microscope to verify surface quality before taking spectroscopic measurements is used to remove the effects of defect scattering on experimental lifetimes, found to have been a significant contribution to prior determinations. A theoretical treatment of inelastic electron-electron scattering is developed that explicitly includes intraband transitions within the surface state band. In our model, two-dimensional decay channels dominate the electron-electron interactions that contribute to the hole decay and are screened by the electron states of the underlying three-dimensional electron system.

A fundamental concept in condensed matter physics is the notion of a quasiparticle, an elementary excitation of an interacting Fermi liquid. The interactions between quasiparticles limit how long the corresponding quantum states retain their identity: a quasiparticle is said to have a lifetime, which sets the duration of the excitation. Furthermore, in combination with the velocity, this lifetime determines the mean free path of the quasiparticle, a measure of the range of influence of the excitation. Thus, the quasiparticle lifetime enters the description of many important phenomena, such as the dynamics of charge and energy transfer; screening in an electron gas and the Friedel oscillations; electron-phonon coupling, the cornerstone of conventional superconductivity; localization; quantum interference; and many more.

In metallic systems, two-dimensional (2D) quasiparticle states—states that are localized in one of the three spatial directions—are of natural and increasing importance in surface science (1) and in nanoscale technology (2). In these systems, the situation is generally both more complex and less well understood compared with more homogeneous three-dimensional (3D) (3) and 2D (4) systems, even when the states in question are readily accessible to experiment. This applies to the surface electronic states that have been observed on the faces of many crystals (1,

5–10), 2D states that overlap in energy and space with 3D states and produce interesting possibilities for quasiparticle decay to proceed simultaneously through both 2D and 3D channels (Fig. 1), whilst the quasiparticles are stabilized through 3D screening, which may involve energetically well-separated levels. Despite prolonged experimental and theoretical effort [reviewed in (11)], the lifetime of one of the simplest quasiparticles, a hole in such a surface state band, remains unclear. Theoretical models predict significantly longer lifetimes than are observed with photoelectron spectroscopy (PES)—differing by as much as a factor of 8 for Au(111). As a result, the surface state lifetime has achieved a wider importance in the context of understanding quasiparticle interactions (12).

We present experimental data collected with a scanning tunneling microscope (STM) and a model for electron-electron scattering, in an effort to address this discrepancy. The STM enables defect scattering to be eliminated, and we are able to report increased experimental lifetimes. Our calculations show that important screening corrections had been overlooked previously, and thus the electron-electron scattering rate was significantly underestimated due to neglect of the dominant contribution of intraband transitions within the 2D surface state band.

Our experiments were performed with an in-house built ultra-high vacuum (UHV) low-temperature STM (13) operating at 4.6 K, using electrochemically etched W tips that were further prepared in UHV by heating and Ar⁺ bombardment. Samples of the (111) faces of Ag, Au, and Cu crystals were prepared in UHV by standard cycles of sputtering and annealing. With the STM, large defect-free regions of the surfaces were identified, and their electronic structure was studied by *dI/dV* differential conductance spectroscopy,

which measures a quantity that approximates the density of electronic states at the surface. From the experimental data (Fig. 2), where the *dI/dV* spectra have been averaged over experiments with many different STM tips (14), the surface states appear as a prominent rise at *V* = −67, −505, and −445 mV for Ag, Au, and Cu, respectively, reflecting the threshold for tunneling from the partially occupied surface state band.

Previous work (15) has shown that the width of this onset in Fig. 2, Δ , is directly related to the lifetime of holes at the surface state band-edge

$$\tau = \beta \frac{h}{4\Delta} \quad (1)$$

where *h* is Planck's constant and β is a factor close to unity that measures the extent to which the tunneling state couples to lifetime-limiting processes. To identify values of τ , we determine β for these noble metal surface states with the method previously described (15). Current-voltage characteristics are calculated for each of the surfaces with a many-body tunneling theory implemented within a multiple-scattering framework, and the calculations are numerically differentiated to obtain *dI/dV* spectra. These are then analyzed to determine the proportionality between Δ and a local uniform imaginary self-energy within the solid. Analyzing the data from Fig. 2, we then arrive at lifetimes of $\tau = 120, 35$, and 27 fs for the states at the surface-state band edge on Ag, Au, and Cu, respectively (Table 1) (16).

An important asset of STM is that surface quality can be verified before performing spectroscopic measurements. This is in con-

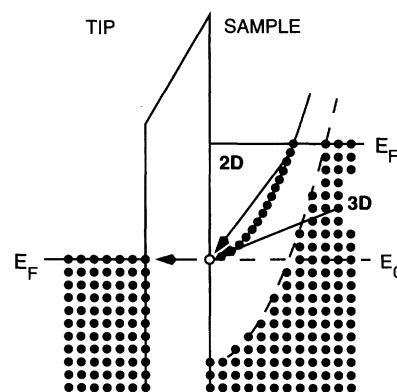


Fig. 1. Schematic energy diagram for an electron (electrons shown as solid circles) tunneling from the bottom (E_0) of an occupied surface band (solid parabola) of the sample to a metallic tip. States in the sample are displayed as a projected band structure. The dashed parabola indicates the maximum of the bulk bands. Fermi energies are denoted E_F . The hole (open circle) left behind by a tunneling electron is filled by an intraband transition (arrow 2D) or a bulk state (arrow 3D).

¹RWTH Aachen, II. Physikalisches Institut, D-52056 Aachen, Germany. ²Institut für Experimentelle und Angewandte Physik, Christian-Albrechts-Universität zu Kiel, D-24098 Kiel, Germany. ³Departamento de Física de Materiales, Facultad de Química, Universidad del País Vasco and Centro Mixto UPV-CSIC and Donostia International Physics Center, Apdo. 1072, 20080 San Sebastian, Spain. ⁴Department of Physics, University of Bath, Bath, BA2 7AY, UK.

*To whom correspondence should be addressed. E-mail: berndt@physik.uni-kiel.de

trast to PES, which historically has been the principal tool for studying surface states. In PES, radiation incident on the metal surface illuminates a region typically 10^2 to 10^3 μm across, which contains an unknown distribution of surface defects. Defects are known to strongly couple the surface state electrons to bulk states and thus reduce lifetimes (17). With PES it is conventional to discuss not the lifetime but the line width $\Gamma = \hbar/\tau$ of the associated transition in which an electron in the surface state band absorbs a photon and is ejected from the sample (11). In Table 1, we compare line widths obtained from our STM measurements with previous PES data. For Ag(111) and Au(111), STM measures line widths smaller by a factor of 3 than PES (i.e., longer lifetimes), illustrating how large the electron-surface imperfection scattering contribution is. For Cu(111), the situation is markedly different. In this case, the PES value of 21 meV has been obtained by exploiting an observed correlation with low-energy electron diffraction spot profiles (18) to extrapolate the PES line width to zero defect density. The good agreement here with the STM value provides evidence to support the use of this novel procedure for removing defect-induced broadening in PES.

Eliminating the defect-scattering contribution partially improves agreement between experiment and theory, but a large discrepancy remains. Table 1 lists theoretical values of Γ_{old} based on previous theory. In the absence of defect scattering, two processes limit the lifetime of the hole: inelastic electron-electron scattering and electron-phonon coupling. Previous estimates of the former have assumed 3D decay channels dominate, with the hole filled by interband transitions involving the bulk electrons near the surface, and have calculated the line width using the degenerate electron gas model (DEGM) of an isotropic Fermi liquid (3). Also included in the value listed in Table 1 is the screening contribution of the d -electrons [(19); discussed below]. The importance of the phonon contribution was only recently identified (20) and was used to successfully describe the temperature dependence of the line width of the Cu(111) surface state in terms of the electron-phonon scattering rate evaluated using the bulk Debye model for the spectral density of the electron-phonon coupling $\alpha^2 F(\omega)$ (21). The Γ_{old} values listed in Table 1 include contributions of 5.2, 5.2, and 8 meV for Ag, Au, and Cu, respectively (22), which we calculated with this approach. Surface effects lead only to minor corrections of these numbers (23), indicating that the electron-phonon scattering contribution is not sensitive to the dimensionality, whilst the fact that the surface state band edges of the noble metals lie at ener-

Table 1. Summary of measured and calculated lifetimes and line widths of the band-edge surface state on the (111) faces of the noble metals. The lifetime τ is obtained from the differential conductance spectra obtained with the STM, combining measured lineshape parameters Δ (Fig. 2) with proportionality constants β determined from tunneling theory. Γ_{STM} is the corresponding line width \hbar/τ . Γ_{PES} denotes the line width previously determined by PES. These are to be compared with theoretical values. Γ_{old} denotes the line width in the degenerate electron gas model, and Γ_{new} denotes the present calculation, including band structure and surface effects. Both of these calculations include d -screening in the electron-electron scattering and electron-phonon scattering as calculated within a 3D Debye model.

Metal	Δ (meV)	β	τ (fs)	Experiment		Theory	
				Γ_{STM} (meV)	Γ_{PES} (meV)	Γ_{old} (meV)	Γ_{new} (meV)
Ag	8	0.89	120	6	20*	5.3	7.2
Au	23	0.82	35	18	60†	8.6	18.9
Cu	30	0.80	27	24	21‡	10.2	21.7

* (17) † Extrapolation down to $T = 0$ K of data from (30).

‡ (18).

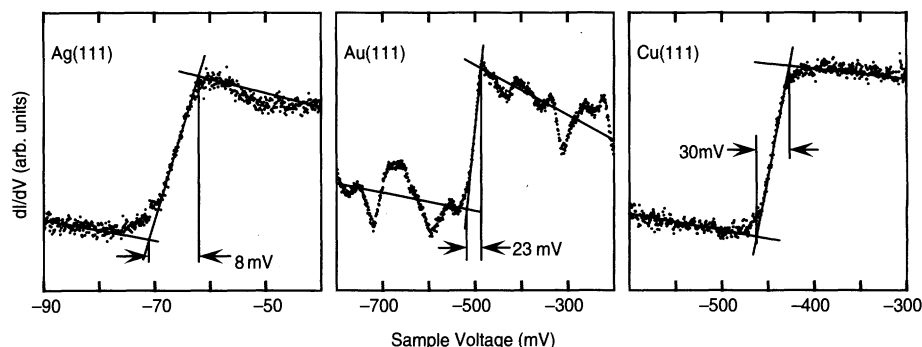


Fig. 2. dI/dV spectra for Ag(111), Au(111), and Cu(111). All spectra were taken at least 200 Å away from impurities and are averages of different single spectra from varying sample locations and tips. In particular, the Au(111) spectrum constitutes an average over 17 single spectra taken across various positions across the surface reconstruction.

gies well below the maximum phonon frequency and that the phonon spectrum enters in integral form (22, 23) also means that these values are rather insensitive to the precise form of the $\alpha^2 F(\omega)$; consequently, the use of the Debye spectrum is not expected to be a large source of error. We are therefore led to conclude that the discrepancy between theory and experiment originates in the evaluation of the inelastic electron-electron contribution.

In the new treatment we report, both band structure and surface effects are included, so that we correctly include both 2D and 3D decay processes in describing the lifetime of the holes in the surface state band. The electron-electron scattering contribution to the inverse-lifetime or line width of a quasiparticle with energy E is evaluated as a projection of the imaginary part of the quasiparticle self-energy, $\Sigma(\mathbf{r}, \mathbf{r}'; E)$, over the state itself. We calculate this self-energy with the GW approximation of many-body theory (24), retaining the first term in the series expansion of Σ in terms of the screened Coulomb interaction W . Replacing the full Green function G by the noninteracting Green function, we obtain the following contribution to the line width of the surface state at the band edge energy E_0 (25)

$$\Gamma_{e-e} = -2 \sum_{n, \mathbf{k}_{\parallel}} \int d\mathbf{z} \int d\mathbf{z}' \varphi_0^*(z) \varphi_n(z') \times \text{Im} W(z, z'; \mathbf{k}_{\parallel}; E_{n\mathbf{k}_{\parallel}} - E_0) \varphi_n(z) \varphi_0(z'). \quad (2)$$

The sums over bands n and surface momenta \mathbf{k}_{\parallel} include all states lying in energy between the surface state energy and the Fermi level, E_F , where $\varphi_n(z)$ is the corresponding wave function normal to the surface and φ_0 refers to the surface state. The screened interaction W is found from the density response function that we evaluate in the random-phase approximation (RPA) (25).

The wave functions φ_n and φ_0 entering Eq. 2 are calculated with a well-tested potential (26) that exactly reproduces the width and position of the energy gap, as well as the binding energies of the surface state and the first image state at the center of the surface Brillouin zone. This pseudopotential correctly reproduces the behavior of the s - p valence states around E_F , ensuring that Γ_{e-e} from Eq. 2 accurately includes all inter- and intraband transitions of that part of the surface electronic structure where d -states are not significant. Transitions involving the d -states are not expected to play a direct role here because the noble metal d -bands lie rather deep in energy.

Table 2. The inelastic electron-electron scattering energy contribution to the line width Γ_{e-e} of a hole at the surface-state band edge, as obtained from the DEGM and this report, with and without d -electron screening corrections. Values in parentheses denote the contribution from intraband transitions within the surface state band.

Surface	Energy (meV)	DEGM		Present theory	
		No d -scr.	d -scr.	No d -scr.	d -scr.
Ag(111)	-67	0.1	≈ 0.1	3 (2.7)	2.0 (1.8)
Au(111)	-505	8.8	3.4	29 (21)	13.7 (10.6)
Cu(111)	-445	5.1	2.2	25 (19)	13.7 (11.1)

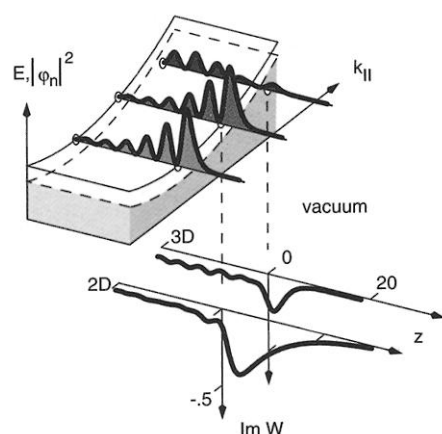


Fig. 3. There is only a gradual evolution in the wave functions $\varphi_n(z)$ of states through the occupied portion of the surface state band, leading to large overlap with the hole wave function φ_0 at the band minimum. In contrast, wave functions associated with levels within the continuum of bulk states exhibit a different spatial distribution near the surface, leading to smaller overlap and making interband transitions less important than intraband transitions in filling the hole. The screened interaction is significantly enhanced near the surface [here $\text{Im}W(z, z)$ is shown, in atomic units], both for 2D intra- and 3D interband transitions, coinciding with where the hole state is concentrated. This results in a hole line width that is much larger than that of bulk states at a similar energy; the hole lifetime is much shorter.

Nevertheless, d -electrons do have an impact on screening and we take their effects into account following an approach proposed by Quinn (19). For excitation energies less than 1 eV, the s - p electrons may be treated as if they are embedded in a polarized medium created by the d -band with a dielectric constant $\epsilon = 1 + \delta\epsilon_d$ instead of unity, and this d -screening reduces the efficiency of transitions into the surface state hole by a factor $\sqrt{\epsilon}$. For energies relevant to our problem, $\delta\epsilon_d$ is practically constant and is equal to 2.4, 5.6, and 4.6 (27) for bulk Ag, Au, and Cu, respectively. By fully screening interband transitions and applying the d -screening correction to intraband transitions within the surface region, we obtain inelastic electron-electron scattering contributions to the

band-edge line widths Γ_{e-e} of 2.0, 13.7, and 13.7 meV for Ag, Au, and Cu, respectively (28).

In Table 2 we compare the predictions of the DEGM with those of the present theory. The DEGM, which assumes 3D transitions and neglects band structure effects, significantly underestimates by factors of 5 to 10 the inelastic electron-electron scattering contributions to the line width. Resolving the transitions in Eq. 2 into interband and intraband contributions, we identify the latter as dominant: The deficiency of the DEGM lies in the neglect of 2D intraband transitions within the surface state band itself, which contribute $\sim 80\%$ to Γ_{e-e} . The 2D \rightarrow 2D transitions are more efficient in filling the hole relative to 3D \rightarrow 2D transitions because of the greater overlap (Fig. 3) of the hole wave function with the occupied states of the surface state band, as compared to the overlap with the bulk states at the surface. The overall larger magnitude of the present estimate of Γ_{e-e} , in which even the contribution from 3D \rightarrow 2D transitions is comparable to the DEGM value that is based upon 3D \rightarrow 3D transitions, arises from weaker screening at the surface, enhancing the screened interaction $\text{Im}W$ in Eq. 2. In addition, the previously omitted screening by d -electrons is seen to provide a significant correction to the overall line width.

In the final column in Table 1, we combine electron-electron and electron-phonon contributions to give total line widths for comparison with the experimental values. Whereas estimates using the DEGM yield values Γ_{old} that are significantly too small, the new calculations (Γ_{new}) are in good agreement with the STM data, so that for the first time a consistent account is found for the hole lifetimes of the noble metal surface states. Scattering by lattice vibrations provides the dominant process limiting the hole lifetimes in Ag, but electron-electron scattering is most important for Au and Cu. Moreover, the previously neglected 2D intraband transitions within the surface state represent a considerable fraction of the total line width. Thus, two-dimensional decay channels dominate the electron-electron interactions that contribute to the hole decay, screened by both s - p

and d electron states of the underlying 3D bulk electron system. At energies above the band edge E_0 , the surface state wave function penetrates deeper into the solid, and the relative importance of the 2D scattering channel is likely to decrease. Nevertheless, recent measurements of unexpectedly short lifetimes of excited electrons on Cu and Ag point to a persisting contribution (29).

These results resolve a long-standing discrepancy in surface science. Furthermore, they open the way to new experimental investigations of electron dynamics in 2D systems that can complement k -space techniques such as ultrafast two-photon PES. The approach we have developed can be extended to study adsorbed atoms, alloys, and thin films, including magnetic multilayers, systems that raise interesting questions concerning electronic coupling and the effects of disorder. The theoretical methods are equally versatile and promise new insight into surface and interface electronic structure.

References and Notes

1. N. Memmel, *Surf. Sci. Rep.* **32**, 91 (1998).
2. F. J. Himpsel, J. E. Ortega, G. J. Mankey, R. F. Willis, *Adv. Phys.* **47**, 511 (1998).
3. J. J. Quinn, *Phys. Rev.* **126**, 1453 (1962).
4. G. F. Giuliani and J. J. Quinn, *Phys. Rev. B* **26**, 4421 (1982).
5. S. D. Kevan and R. H. Gaylord, *Phys. Rev. B* **36**, 5809 (1987).
6. E. W. Plummer and J. B. Hannon, *Progr. Surf. Sci.* **46**, 149 (1994).
7. Y. Hasegawa and Ph. Avouris, *Phys. Rev. Lett.* **71**, 1071 (1993).
8. M. F. Crommie, C. P. Lutz, D. M. Eigler, *Science* **262**, 218 (1993).
9. P. T. Sprunger, L. Petersen, E. W. Plummer, E. Laegsgaard, F. Besenbacher, *Science* **275**, 1764 (1997).
10. P. Hofmann et al., *Phys. Rev. Lett.* **79**, 265 (1997).
11. R. Matzdorf, *Surf. Sci. Rep.* **30**, 153 (1998).
12. N. V. Smith, *Comments Condens. Matter Phys.* **15**, 263 (1992).
13. R. Gaisch et al., *Ultramicroscopy* **42-44**, 1621 (1992).
14. The reconstruction of the Au(111) surface causes some deviation of dI/dV spectra from the expected 2D electron-gas shape (31). However, we verified from series of individual spectra acquired at various sites (fcc, hcp, and domain boundaries) that the width of the rise is not strongly affected.
15. J. Li, W.-D. Schneider, R. Berndt, O. R. Bryant, S. Crampin, *Phys. Rev. Lett.* **81**, 893 (1998).
16. A somewhat shorter lifetime for Ag was reported previously (15). In a new apparatus, we have decreased high-frequency voltage noise at the tunneling tip, which is a source of broadening of dI/dV spectra. Our new, larger value thus represents an improved lower limit of the lifetime.
17. S. Crampin, M. H. Boon, J. E. Inglesfield, *Phys. Rev. Lett.* **73**, 1015 (1994).
18. F. Theilmann, R. Matzdorf, G. Meister, A. Goldmann, *Phys. Rev. B* **56**, 3632 (1997).
19. J. J. Quinn, *Appl. Phys. Lett.* **2**, 167 (1963).
20. B. A. McDougall, T. Balasubramanian, E. Jensen, *Phys. Rev. B* **51**, 13891 (1995).
21. G. Grimvall, *The Electron-Phonon Interaction in Metals* (North-Holland, New York, 1981).
22. We use electron-phonon coupling parameters $\lambda_{\text{Ag}} = 0.13$ (21), $\lambda_{\text{Au}} = 0.17$ (21), and $\lambda_{\text{Cu}} = 0.14$ (20).
23. A strictly 2D Debye model (32) with Debye temperatures determined from the highest surface phonon frequency gives contributions 4.7, 4.7, and 7.6 meV for Ag, Au, and Cu.
24. L. Hedin and S. Lundqvist, *Solid State Phys.* **23**, 1 (1969).

25. E. V. Chulkov, I. Sarria, V. M. Silkin, J. M. Pitarke, P. M. Echenique, *Phys. Rev. Lett.* **80**, 4947 (1998).
26. E. V. Chulkov, V. M. Silkin, P. M. Echenique, *Surf. Sci.* **437**, 330 (1999).
27. E. D. Palik, *Handbook of Optical Constants of Solids* (Academic Press, Boston, 1985).
28. The same approach to d -screening applied to bulk line widths reduces them by a factor of $\epsilon = 2.4$ for Cu. A recent first-principles calculation has shown that d -electrons decrease the line width of bulk states in Cu by a factor of 2.4, in excellent agreement with this model (33).
29. L. Bürgi, O. Jeandupeux, H. Brune, K. Kern, *Phys. Rev. Lett.* **82**, 4516 (1999).
30. S. LaShell, B. A. McDougall, E. Jensen, *Phys. Rev. Lett.* **77**, 3419 (1996).
31. W. Chen, V. Madhavan, T. Jamneala, M. F. Crommie, *Phys. Rev. Lett.* **80**, 1469 (1998).
32. V. N. Kostur and B. Mitrovic, *Phys. Rev. B* **48**, 16388 (1993).

33. I. Campillo, J. M. Pitarke, A. Rubio, E. Zarate, P. M. Echenique, *Phys. Rev. Lett.* **83**, 2230 (1999).
34. J.K. and R.B. thank the Deutsche Forschungsgemeinschaft for support via Sonderforschungsbereich 341. S.C. acknowledges the support of the Engineering and Physical Sciences Research Council. P.M.E. acknowledges the Max Planck Research Award funds. We thank N. Lorente for discussions.

31 January 2000; accepted 5 April 2000

Real-Time Observation of Adsorbate Atom Motion Above a Metal Surface

Hrvoje Petek,*†‡ Miles J. Weida, Hisashi Nagano, Susumu Ogawa

The dynamics of cesium atom motion above the copper(111) surface following electronic excitation with light was studied with femtosecond (10^{-15} seconds) time resolution. Unusual changes in the surface electronic structure within 160 femtoseconds after excitation, observed by time-resolved two-photon photoemission spectroscopy, are attributed to atomic motion in a copper-cesium bond-breaking process. Describing the change in energy of the cesium antibonding state with a simple classical model provides information on the mechanical forces acting on cesium atoms that are "turned on" by photoexcitation. Within 160 femtoseconds, the copper-cesium bond extends by 0.35 angstrom from its equilibrium value.

The observation of atomic and molecular dynamics on surfaces is a long-standing goal in surface science (1–3). Traditional measurements of the energy and momentum deposited in the gas-phase products provide only indirect information on surface processes (4, 5). However, time-resolved spectroscopies using femtosecond-duration laser pulses have finally allowed direct observation of surface dynamics in real time (6). For example, elegant time-resolved photoemission experiments on image potential states have charted coherent surface electron motion and electron trapping and localization by adsorbates (7, 8). Strong excitation-induced coupling between the electrons and nuclei also occurs on a femtosecond time scale; however, to date there has been no equivalent observation of nuclear dynamics on surfaces. The recent discovery of an unusually long-lived electronic state for Cs on Cu(111) (9) makes it possible to record the nuclear motion upon electronic excitation. Here, time-resolved photoemission spectroscopy is used to take a "movie" (13.4 fs per frame) of the change in

Cs/Cu surface electronic structure in the process of breaking the Cu–Cs bond. Inverting this electronic response reveals the real-time dissociative motion of an atom on a surface.

A logical starting point for discussing the photodesorption dynamics is the potential energy surfaces (PESs) for Cs on Cu (Fig. 1A). Despite the fundamental importance of alkali atom chemisorption in catalysis and thermionic emission, only selected aspects of the ground- and excited-state PESs along the Cu–Cs internuclear coordinate ($R_{\text{Cu-Cs}}$) are known (10, 11). The electronic character of the two lowest lying states can be understood from simple atomic orbital ideas. Near a metal, the highest occupied and lowest unoccupied electron orbitals of highly polarizable Cs atoms combine to form a $6s$ – $6p_z$ bonding and $6s$ – $6p_z$ antibonding pair in which the electron density is concentrated at the surface or vacuum side, respectively, of the Cs atom (12, 13). Optical coupling of the ground- and excited-state PESs induces significant charge redistribution about the alkali atom, considerably weakening the Cu–Cs bond (14). Because photoexcitation is much faster than nuclear motion, it projects the ground-state Cs atom probability distribution (wave packet) onto the repulsive wall of the excited state. The ensuing wave packet motion corresponds to the Menzel-Gomer-Redhead scenario for photodesorption (1, 2).

The wave packet evolution can be observed because the $6s$ – $6p_z$ antibonding orbital forms a sharp resonance, which, according to a model

calculation, decreases in energy as $R_{\text{Cu-Cs}}$ increases (13). This electronic change in response to the nuclear motion is recorded by time-resolved two-photon photoemission (2PP) (6, 9). This pump-probe method measures 2PP excited by a pair of identical laser pulses with a

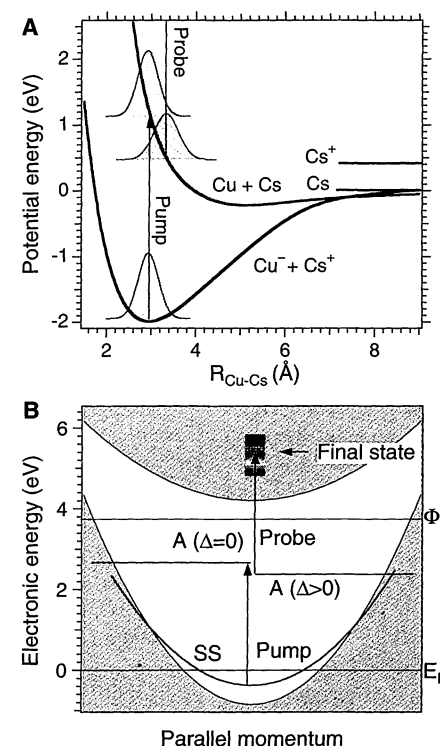


Fig. 1. (A) Schematic PESs are constructed following the procedure in (9). The energy of adsorption of Cs^+ (1.9 eV) and equilibrium $R_{\text{Cu-Cs}}$ (2.97 Å) for the ground state (red) are from thermal desorption (9) and theory (13). The excited state (blue) is constructed with a van der Waals potential for the Cs atoms and a repulsive term that gives the correct excitation energy (5). The asymptotic energies of the Cs^+ and Cs products are indicated by red and blue horizontal lines, respectively (9). The pump pulse projects the ground-state wave packet (represented by a blue gaussian distribution) onto the excited state, "turning on" the repulsive forces. The evolving wave packet (green distribution) is detected by the delayed probe pulse-induced photoemission from the $6s$ – $6p_z$ antibonding state. (B) Band structure for Cu(111), indicating the band gap (unshaded area) and the 2PP excitation scheme. The color gradient for the final state conveys different energies for observation of the dynamics of A. The energy of A decreases approximately quadratically with the delay Δ .

Advanced Research Laboratory, Hitachi, Ltd., Hatoyama, Saitama 350-0395, Japan.

*To whom correspondence should be addressed. E-mail: petek@pitt.edu

†Present address: Department of Chemical Physics, Fritz-Haber Institute, Faradayweg 4-6, D-14195 Berlin, Germany.

‡Permanent address: Department of Physics and Astronomy, University of Pittsburgh, Pittsburgh, PA 15260, USA.